Proceedings of the 9th U.S. National and 10th Canadian Conference on Earthquake Engineering
Compte Rendu de la 9ième Conférence Nationale Américaine et
10ième Conférence Canadienne de Génie Parasismique
July 25-29, 2010, Toronto, Ontario, Canada • Paper No 399

CYCLIC LATERAL-LOAD TEST TO FAILURE OF A FULL-SCALE THREE-STORY FLAT-PLATE REINFORCED CONCRETE STRUCTURE

Damon R. Fick[1]

ABSTRACT

Reinforced concrete flat-plate construction is a popular building type because of the simple formwork required for construction and the clearance provided for mechanical and electrical equipment. The overall earthquake response of flat-plate structures depends on the hysteretic properties of the slab-column connection. The current understanding of the behavior is based largely on the experiments of small-scale isolated slab-column assemblies. The results contain a wide range of maximum drift ratios and failure modes that create uncertainty in evaluation of their behavior during strong ground motion. To evaluate the contributions of multiple stories and connections, a full-scale, three-story reinforced concrete flat plate structure was built and subjected to lateral-load reversals of increasing magnitude. Results of the experimental program show (a) the punching-shear failure of a single slab-column connection was preceded by observable damage in other connections, (b) a lower-bound estimate to the contribution of the slabs to the base shear strength of the three-story flat-plate structure includes the flexural strength of the column strip, and (c) the observed drift limit could be estimated based on projections of limiting drift observed in small scale isolated slab-column connection tests. An expression for limiting story-drift ratio for slab-column connections is presented.

Introduction

The overall earthquake response of flat-plate structures depends on the hysteretic properties of the slab-column connections. The current understanding of the behavior is based largely on the experiments of small-scale isolated slab-column assemblies. The results contain a wide range of maximum drift ratios and failure modes for different specimen geometries, reinforcement ratios, and gravity loading.

A full-scale three-story reinforced concrete structure was built and subjected to lateral-load cycles of increasing magnitude to investigate the effects of multiple stories and connections and to compare the observed drift limit with projections from small-scale isolated specimens.

---

[1]Assistant Professor, Dept. of Civil and Environmental Engineering, South Dakota School of Mines and Technology, 501 East Saint Joseph Street, Rapid City, SD 57701

The experimental program and results are discussed. A comparison with previous research and an estimate for story drift ratio for flat-plate structures are also included.

Cyclic Lateral-Load Test

Test Specimen

The test specimen was a full-scale two-span three-story reinforced concrete flat-plate structure consisting of six columns spaced at 20 ft in each direction supporting a 7 in. thick slab (Figs. 1 and 2). There was a 5 ft cantilevered slab around the perimeter of the building. The footing dimensions were 4 ft-6 in. square by 2 ft-6 in. thick. Each footing was post-tensioned to the 33 in. thick laboratory strong floor with four 1-3/8 in. Dywidag Threadbars ®, each post-tensioned to 100 kips. Also shown in Figs. 1 and 2 are the floor levels and Frame locations, which are used to identify specific slab-column connections. Details of the design, construction, and instrumentation of the specimen are described by Fick (2008).

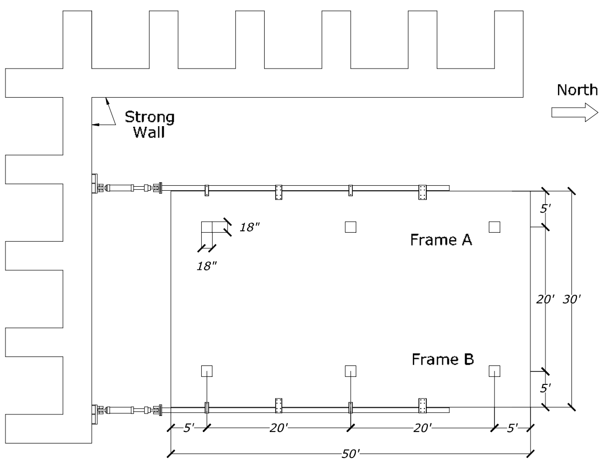

Figure 1. Specimen plan view.

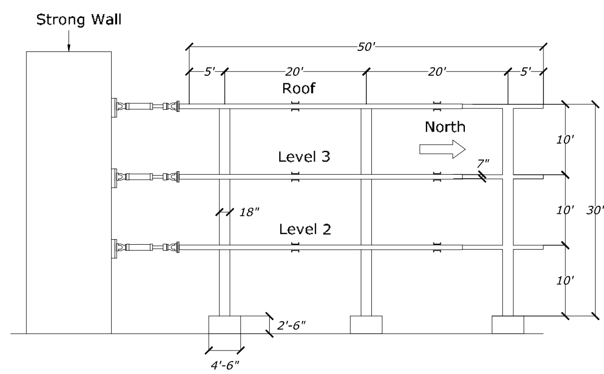

Figure 2. Specimen elevation view.

Testing Program

Six 110-kip hydraulic actuators (2 per floor) were used to apply lateral load to the test structure. The actuators were connected to a strong wall and applied load to each floor level through a steel load frame bolted to the slab (Fick 2008). The test was controlled by the two roof-level actuators operating in displacement control. The load from these actuators was used to control the actuators on Level 3 and Level 2 in load control such that the forces applied related to the “linear mode shape.” Fig. 3 is a schematic showing the applied load distribution and the control strategy.

A superimposed load was added to the structure by filling 55 gallon barrels with water. Each barrel weighed approximately 500 lbs. Forty barrels per floor resulted in a distributed load of 13.3 psf. Total weight of the building, including the superimposed loading was 509 kips. A photograph of the completed specimen, distributed loading, and steel load frame is shown in Fig. 4.

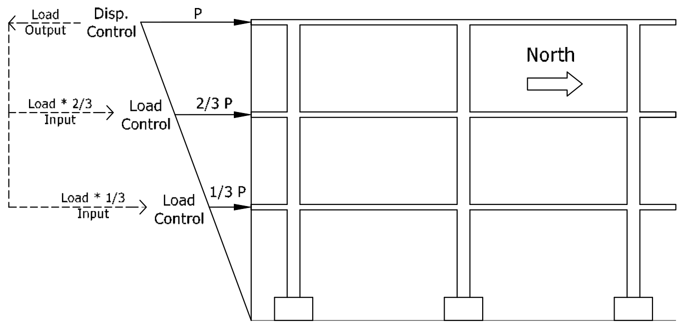

Figure 3. Load distribution and control schematic

Figure 4. Completed specimen with load frames and water barrel loading.

The cyclic lateral-load test included four cycles of loading. Each cycle began loading in the north direction, followed by loading in the south direction to complete the cycle. Values of displacements and loads are positive for loading in the north direction (Fig. 3). Loading was paused at each of the target displacements and at intermediate loading points during cycles 3 and 4 to observe and document the response of the structure.

Table 1 is a summary of the load and displacements measured during each cycle of loading. Fig. 5 is a plot of the base shear vs. roof displacement for each cycle of loading.

Table 1. Experimental Program Summary

	Maximum Values					
	Base Shear, kips		Base Shear	Roof Disp., in.		Roof
	North	South	Coeff., C_b	North	South	Drift, %
1st Cycle	52	-54	0.11	0.68	-0.70	0.2
2nd Cycle	80	-80	0.16	1.51	-1.51	0.4
3rd Cycle	137	-134	0.27	5.41	-5.41	1.5
4th Cycle	161	-154	0.32	10.81	-10.83	3.0

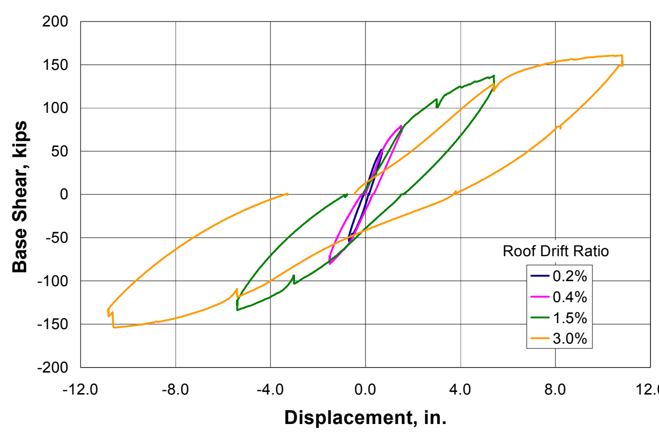

Figure 5. Base shear vs. roof displacement

Load Test Observations at Limiting Drift

A local failure occurred at the slab-column connection in Frame B shown in Fig. 6 during loading in the south direction of cycle 4. The story shears and displacements immediately before the failure are shown in Table 2. The roof displacement at failure was 10.5 in. (2.9% roof drift ratio). The peak base shear was 154 kips (base shear coefficient, $C_b = 0.30$). The failure occurred suddenly without any forewarning in the load-displacement curve. On its occurrence, the measured base shear dropped 18 kips to 136 kips ($C_b = 0.27$). Loading in the south direction was resumed 4 minutes later until the roof displacement was 10.8 in (3.0% roof drift ratio). The corresponding base shear was 140 kips ($C_b = 0.28$). Photographs of the failure are shown in Fig. 7.

Table 2

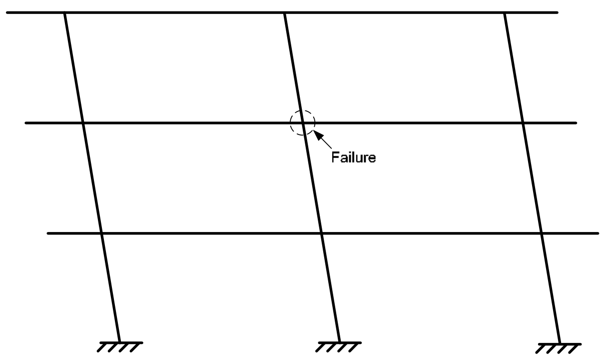

Figure 6. Frame B failure location.

Level	Shear [kips]	Story Shear [kips]	Disp. [in]	Story Disp. [in]	Roof Drift [%]	Story Drift [%]
3	76.9	25.6	10.54	3.70	2.93	3.08
2	51.3	103	6.84	3.97		3.31
1	25.6	154	2.87	2.87		2.39

Figure 7. Slab column connection failure.

In cycle 4 when the displacement reached the maximum loading to the north, vertical separations of the slab near the columns ranging from 1/16 to 5/16-in. on both the bottom and top surfaces of the slab were observed, but there had been no indication of it in the load-displacement curve. The locations and depths of these measurements are shown in Fig. 8.

Vertical slab separations were also observed near the columns at the target displacement in the south direction (after failure). Slab separations near the columns ranged from 1/16 to 1/2-in. and are shown in Fig. 9. Representative photographs of the observed vertical slab separations are shown in Fig. 10.

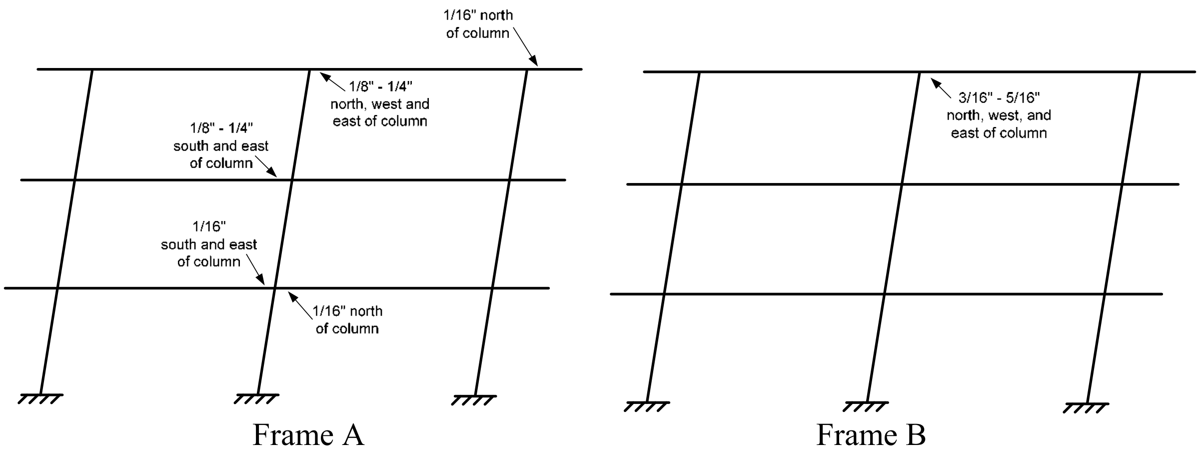

Figure 8. Vertical slab separations in north loading of Cycle 4.

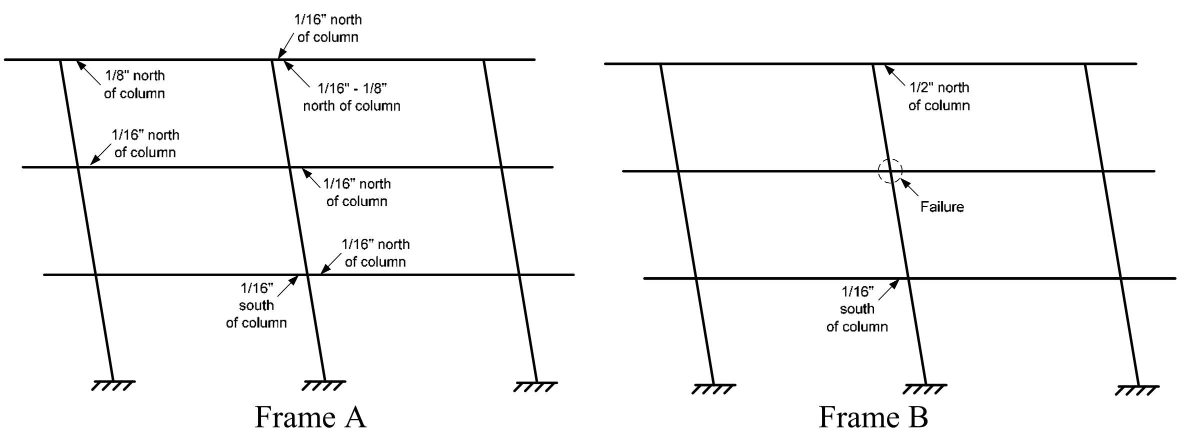

Figure 9. Vertical slab separations in south loading of Cycle 4.

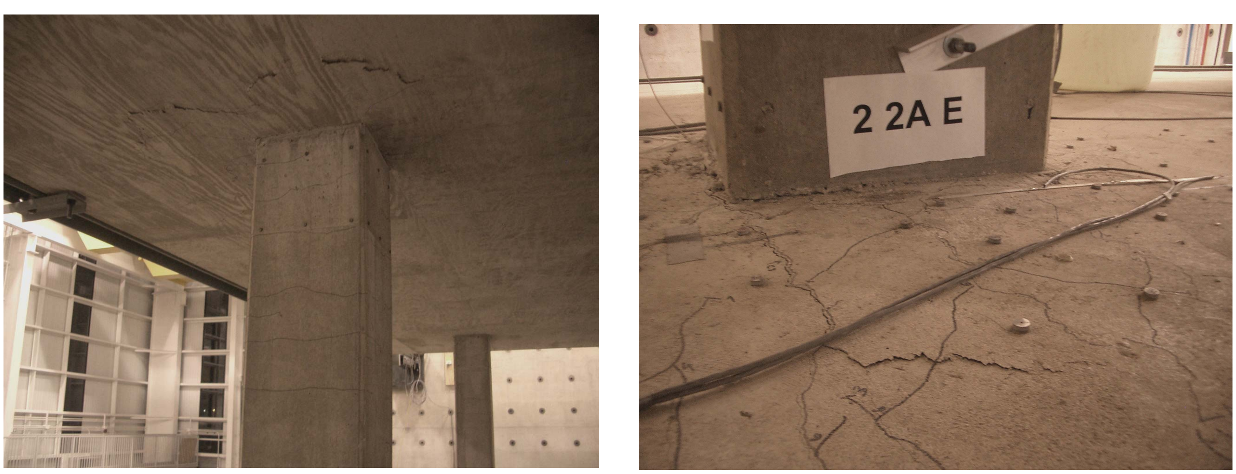

Figure 10. Vertical slab separations before limiting drift condition.

Vertical slab separations in Frame A at the peak loading in the north direction were observed in four different slab-column connections compared with one location in Frame B (Fig. 8). Three of these vertical separations were observed at the center column of Frame A. In addition to the separations in this column, the crack widths at level 2 and 3 of the north column in Frame A were 50% larger than the crack widths at the same location in Frame B, where fewer vertical separations were observed. The observations suggest damage in the slab surrounding the center column of Frame A was driven by the rotation demand at the slab-column connections to the north column of Frame A. The redistribution of rotations continued while loading in the south direction of cycle 4 and contributed to the slab-column connection failure in Frame B (Fig. 9).

Analysis

Limit State Analysis

A limit state analysis was used to approximate the base shear capacity of the flat-plate structure. The magnitude of the base shear is found by setting the work done by the external loads equal to the internal work by the frame members. The assumed failure mechanism and loading used in the limit state analysis are shown in Fig. 11.

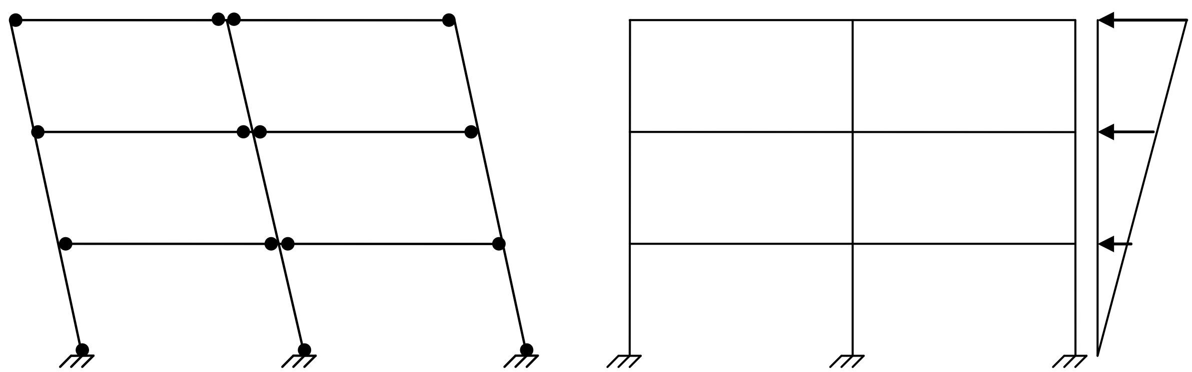

(a) (b)

Figure 11. Assumed failure mechanism (a) and loading (b) for limit state analysis

Base shear coefficients calculated using strengths of the entire slab width (15 ft) and the column strip (10 ft) are shown with the envelope of the flat-plate test data in Fig. 12. The measured strength of the flat-plate test structure was between the two values. Because the 15 ft width is asymmetric about the column and because it is preferable to underestimate the base shear strength in design analyses, a slab width of 10 ft is selected as a lower bound moment capacity of the slab-column connections.

Evaluation of Small-Scale Data

An incentive for testing the full-scale flat-plate structure was to compare the results with previous investigations of small-scale isolated slab-column specimens (Table 3). The effects of slab-column connections in multiple stories and frames to the failure of a single connection make the comparison useful.

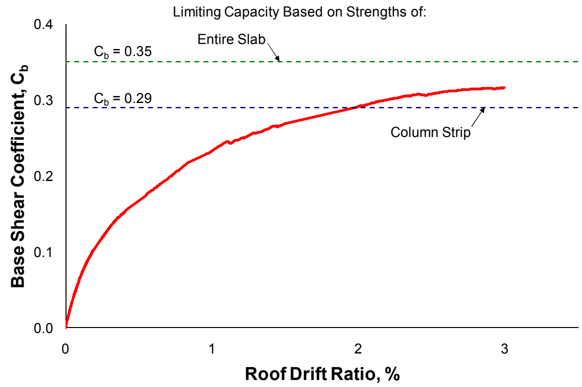

Figure 12. Limit state analysis results

The isolated test assemblies represent slab-column connections of a prototype structure. The peak drifts of these specimens are compared with the second story drift ratio of the full-scale specimen, which was 3.4%, recorded at the level of the connection failure.

A trend of reduced drift in slab-column connections has been observed for higher gravity-shear ratios (Pan and Moehle 1989; 1992). The gravity shear on the flat-plate structure includes 87.5 psf self weight and 13.3 psf superimposed loading. This loading distributed over the tributary area of an interior column (300 ft^2) produces 30 kips of shear at the connection. The assumed critical section for the flat-plate test structure is the perimeter a distance of d/2 from the column (576 in^2) which provides a nominal shear capacity of 146 kips for a condition of no moment transfer (ACI 318-08) From these values, the gravity-shear ratio, γ , for the flat-plate structure is calculated to be 0.2.

Results of the available tests of slab-column connections (Table 3) are plotted in Fig. 13. The y-axis is the gravity shear ratio, γ, the x-axis is the story drift ratio, SDR. The story drift limit is well within the trend of the data.

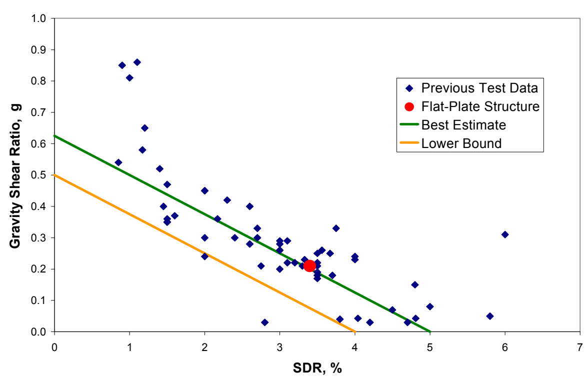

Figure 13. Flat-plate comparison with previous data.

It is interesting and relevant to note that a "best estimate" representative of the data would be the simple expression shown in Eq. 1. A safe "lower-bound" that would be suitable for design is shown in Eq. 2.

Table 3. Experimental Programs

	Label	γ	Peak Drift [%]	Failure	Test Moment [k-in]
(Durrani et al. 1995)	DNY 1	0.20	3.0	F	220
	DNY 2	0.30	2.0	P	194
	DNY 3	0.24	2.0	F	206
	DNY 4	0.28	2.6	F-P	220
(Elgabry and Ghali 1987)	1	0.46	N/A	P	1152
(Farhey et al. 1993)	1	0.04	4.8	F	292
	2	0.04	4.0	F	292
	3	0.26	3.6	P	168
	4	0.30	2.4	P	133
(Ghali et al. 1976)	SM 0.5	0.31	6.0	F	888
	SM 1.0	0.33	2.7	F-P	1128
	SM 1.5	0.30	2.7	F-P	1176
(Hanson and Hanson 1968)	A12	0.29	N/A	P	181
	A13L	0.29	N/A	P	176
	B16	0.29	N/A	P	242
	B7	0.04	3.8	F-P	316
	C17	0.24	N/A	F-P	219
	C8	0.05	5.8	F	278
(Hawkins et al. 1974)	S1	0.33	3.8	P	1280
	S2	0.45	2.0	P	778
	S3	0.45	2.0	P	475
	S4	0.40	2.6	P	1110
(Hwang and Moehle 2000)	4 Int. Joints	0.24	4.0	N/A	N/A
(Islam and Park 1976)	1	0.25	3.7	P	270
	2	0.23	3.3	P	334
	3C	0.23	4.0	F-P	317
(Robertson and Johnson 2006)	ND1C	0.23	3.0 to 5.0	F-P	375
	ND4LL	0.28	3.0	F-P	394
	ND5XL	0.47	1.5	P	288
	ND6HR	0.29	3.0	P	519
	NC7LR	0.26	3.0	F-P	265
	ND8BU	0.26	3.0	F-P	520
(Luo and Durrani 1995)	I.I	0.08	5.0	F	348
	INT 1	0.43	N/A	P	347
	INT 2	0.50	N/A	P	280
(Megally and Ghali 2000)	MG-2A	0.58	1.2	P	576
	MG-7	0.29	3.1	F-P	641
	MG-8	0.42	2.3	F-P	679
	MG-9	0.36	2.2	F-P	758
(Morrison et al. 1983)	S1	0.03	4.7	F	302
	S2	0.03	2.8	F	343
	S3	0.03	4.2	F	363
	S4	0.07	4.5	F	314
	S5	0.15	4.8	F	332
(Pan and Moehle 1989)	AP 1	0.37	1.6	F-P	468
	AP 2	0.36	1.5	F-P	396
	AP 3	0.18	3.7	F-P	720
	AP 4	0.19	3.5	F-P	684
(Pan and Moehle 1992)	1	0.35	1.5	P	468
	2	0.35	1.5	P	396
	3	0.22	3.1	F-P	720
	4	0.22	3.2	P	684
(Robertson and Durrani 1990)	1	0.21	2.8	F	573
	2C	0.22	3.5	F-P	586
	3SE	0.19	3.5	F	640
	5SO	0.21	3.5	F	591
	6LL	0.54	0.9	P	227
	7L	0.40	1.5	P	353
	8I	0.18	3.5	F-P	590
(Robertson et al. 2002)	1C	0.17	3.5	P	517
(Symonds et al. 1976)	S6	0.86	1.1	P	644
	S7	0.81	1.0	P	376
(Wey and Durrani 1992)	SC 0	0.25	3.5	P	549
(Zee and Moehle 1984)	INT	0.21	3.3	F-P	N/A

$$SDR(\%) = 5 - 8\gamma \quad (1)$$
$$SDR(\%) = 4 - 8\gamma \quad (2)$$

where:

γ = gravity shear ratio, $V_g/V_o < 0.5$

V_g = gravity shear carried by slab-column connection

V_o = nominal shear capacity for slab-column connection defined by the current ACI Building Code (ACI 318-08).

Summary and Conclusions

A full-scale three-story reinforced concrete flat-plate structure was built and subjected to lateral-load reversals of increasing magnitude. A superimposed load of 13.3 psf was placed on the structure to represent a permanent loading condition for a typical building. The self weight of the slab was 87.5 psf. Four cycles of loading produced roof drift ratios of 0.2, 0.4, 1.5, and 3.0%. Based on experimental observations of the full-scale flat-plate test structure, the following is concluded:

1.) Initiation of failure at slab-column connections was indicated by small changes (1/16 to 5/16 in.) in elevation of the slab near the column. The damage observed before the limiting drift condition did not result in complete failure of an individual slab-column connection because of the inherent redundancy of the three-story flat-plate structure.

2.) A lower-bound estimate to the contribution of the slabs to the base shear strength of the three-story flat-plate structure includes the flexural strength of the column strip (10 ft.)

3.) The observed drift limit of the three-story flat plate structure could be reasonably estimated based on projections of limiting drift observed in small scale isolated slab-column connection tests.

4.) A lower bound to the limiting story drift ratio (SDR) for slab-column connections can be estimated by Eq. 2:

$$SDR(\%) = 4 - 8\gamma \quad (2)$$

where γ = gravity shear ratio

Acknowledgments

The investigation described here was carried out at Bowen Laboratory for Large-Scale Testing , Purdue University, with support from the U.S. Army's Construction Engineering Laboratory, Hunt Construction, and Jack and Kay Hockema, and the Kettelhut Grant. Appreciation is due Dr. Jack Hayes and Mr. James Wilcoski for their encouragement and advice during the planning of the tests.

References

ACI Committee 318 (2008). *Building Code Requirements for Structural Concrete (ACI 318-08) and Commentary (ACI 318R-08)*, American Concrete Institute, Farmington Hills, MI.

Durrani, A. J., Du, Y., and Luo, Y. H. (1995). "Seismic Resistance of Nonductile Slab-Column Connections in Existing Flat-Slab Buildings." *ACI Structural Journal*, 92(4), 479-487.

Elgabry, A. A., and Ghali, A. (1987). "Tests on Concrete Slab-Column Connections with Stud-Shear Reinforcement Subjected to Shear-Moment Transfer." *ACI Structural Journal (American Concrete Institute)*, 84(5), 433-442.

Farhey, D. N., Adin, M. A., and Yankelevsky, D. Z. (1993). "RC Flat Slab-Column Subassemblages Under Lateral Loading." *Journal of Structural Engineering*, 119(6), 1903-1916.

Fick, D. R. (2008). "Experimental Investigation of a Full-Scale Flat-Plate Reinforced Concrete Structure Subjected to Cyclic-Lateral Loading in the Inelastic Range of Response," Dissertation, Purdue University, West Lafayette, IN.

Ghali, A., Elmasri, M. Z., and Dilger, W. (1976). "Punching of Flat Plates Under Static and Dynamic Horizontal Forces." *Journal of The American Concrete Institute*, 73(10), 566-572.

Hanson, J. M., and Hanson, N. W. (1968). "Shear and Moment Transfer Between Concrete Slabs and Columns." *Portland Cement Association -- Research and Development Laboratories -- Journal*, 10(1), 2-16.

Hawkins, N. M., Mitchell, D., and Sheu, M. S. (1974). "Cyclic Behavior of Six Reinforced Concrete Slab-Column Specimens Transferring Moment and Shear." *Progress Report, NSF Project GI-38717*, University of Washington, Seattle, WA.

Hwang, S.-J., and Moehle, J. P. (2000). "Vertical and Lateral Load Tests of Nine-Panel Flat-Plate Frame." *ACI Structural Journal*, 97(1), 193-203.

Islam, S., and Park, R. (1976). "Tests on Slab-Column Connections with Shear and Unbalanced Flexure." 102(3), 549-568.

Luo, Y. H., and Durrani, A. J. (1995). "Equivalent Beam Model for Flat-Slab Buildings - Part I: Interior Connections." *ACI Structural Journal*, 92(1), 115-124.

Megally, S., and Ghali, A. (2000). "Punching of Concrete Slabs Due to Column Moment Transfer." *Journal of Structural Engineering*, 126(2), 180-189.

Morrison, D. G., Hirasawa, I., and Sozen, M. A. (1983). "Lateral-Load Tests of R/C Slab-Column Connections." *Journal of Structural Engineering*, 109(11), 2698-2714.

Pan, A., and Moehle, J. P. (1989). "Lateral Displacement Ductility of Reinforced Concrete Flat Plates." *ACI Structural Journal (American Concrete Institute)*, 86(3), 250-258.

Pan, A. D., and Moehle, J. P. (1992). "Experimental Study of Slab-Column Connections." *ACI Structural Journal (American Concrete Institute)*, 89(6), 626-638.

Robertson, I., and Durrani, A. J. (1990). "Seismic Response of Connections in Indeterminate Flat-Slab Subassemblies." *41*, Rice University, Houston, TX.

Robertson, I., and Johnson, G. (2006). "Cyclic Lateral Loading of Nonductile Slab-Column Connections." *ACI Structural Journal*, 103(3), 356-364.

Robertson, I. N., Kawai, T., Lee, J., and Enomoto, B. (2002). "Cyclic Testing of Slab-Column Connections with Shear Reinforcement." *ACI Structural Journal*, 99(5), 605-613.

Symonds, D. W., Mitchell, D., and Hawkins, N. M. (1976). "Slab-Column Connections Subjected to High Intensity Shears and Transferring Reversed Moments." *Progress Report on NSF Project GI-38717*, University of Washington, Seattle, WA.

Wey, E. H., and Durrani, A. J. (1992). "Seismic Response of Interior Slab-Column Connections with Shear Capitals." *ACI Structural Journal (American Concrete Institute)*, 89(6), 682-691.

Zee, H. L., and Moehle, J. P. (1984). "Behavior of Interior and Exterior Flat Plate connections Subjected to Inelastic Load Reversals." *Earthquake Engineering Research Center No.UCB/EERC-84/07*, University of California, Berkeley, CA.